Palaeogeography, Palaeoclimatology, Palaeoecology 311 (2011) 268–280

Contents lists available at SciVerse ScienceDirect

Palaeogeography, Palaeoclimatology, Palaeoecology

journal homepage: www.elsevier.com/locate/palaeo

Arctic front shifts in the subpolar North Atlantic during the Mid-Pleistocene (800–400 ka) and their implications for ocean circulation

Montserrat Alonso-Garcia *, Francisco J. Sierro, José A. Flores

Department of Geology (Paleontology), University of Salamanca, Pza. de la Merced s/n, 37008, Salamanca, Spain

A R T I C L E I N F O

Article history:
Received 26 January 2011
Received in revised form 27 August 2011
Accepted 11 September 2011
Available online 17 September 2011

Keywords:
Planktic foraminifers
Subpolar North Atlantic
Arctic front
Sea ice extent
Factor analysis
Mid-Pleistocene

A B S T R A C T

Surface water conditions at the Integrated Ocean Drilling Program (IODP) Site U1314 (Southern Gardar Drift, 56° 21.8′ N, 27° 53.3′ W, 2820 m depth) were inferred using planktic foraminifer assemblages between Marine Isotope Stage (MIS) 19 and 11 (ca. 800–400 ka). Factor analysis of the planktic foraminifer assemblages suggests that the assemblage was controlled by three factors. The first factor (which explained 49% of the variance) is dominated by transitional and subpolar species and points to warm and salty surface water conditions (Atlantic water). The second factor (37%) is dominated by *Neogloboquadrina pachyderma* sin and has been associated with the presence of cold and low saline surface waters (Arctic water). Finally, the third factor (9%), linked to a significant presence of *Turborotalita quinqueloba*, reflects the closeness of the Arctic front (the boundary between Atlantic and Arctic water). The position of the Arctic and Polar fronts has been estimated across the glacial–interglacial cycles studied according to planktic foraminifer abundances from Site U1314 (and their factor analysis) combined with a synthesis of planktic foraminifer and diatom data from other North Atlantic sites. Regarding at the migrations of the Arctic front and the surface water masses distribution across each climatic cycle we determined five phases of development. Furthermore, deep ocean circulation changes observed in glacial–interglacial cycles have been associated with each phase.

The high abundance of transitional-subpolar foraminifers (above 65% at Site U1314) during the early interglacial phase indicated that the Arctic front position and surface water masses distribution were similar to present conditions. During the late interglacial phase, *N. pachyderma* sin and *T. quinqueloba* slightly increased indicating that winter sea ice slightly expanded southwestwards whereas the ice volume remained stable or was still decreasing. *N. pachyderma* sin increased rapidly (above 65% at Site U1314) at the first phase of glacial periods indicating the expansion of the Arctic waters in the western subpolar North Atlantic. During the second phase of glacial periods the transitional-subpolar assemblage throve again in the central subpolar North Atlantic associated with strong warming events that followed ice-rafting events. The third phase of glacial periods corresponds to full glacial conditions in which *N. pachyderma* sin dominated the assemblage for the whole subpolar North Atlantic. This division in phases may be applied to the last four climatic cycles.

1. Introduction

Changes in thermohaline circulation (Broecker and Peng, 1989; Broecker, 1991), particularly in the Atlantic Ocean, have been thoroughly studied during the last 3–4 decades. In the modern ocean and during interglacial periods, the production of North Atlantic deep water (NADW) maintained active the Atlantic Meridional Overturning Circulation (AMOC). NADW is mainly generated through open ocean convection in the Norwegian Greenland Sea (NGS) and Labrador Sea (Schmitz and McCartney, 1993), where the warm and high salinity water of the North Atlantic current (NAC) gets denser by releasing heat to the atmosphere and sinks. Conversely, during glacial periods deep sea sediments suggest that the AMOC was reduced and the Southern Ocean water filled the deep Atlantic ocean replacing the NADW at depths below ~2000–2200 m (Boyle and Keigwin, 1982; Curry and Lohmann, 1983; Boyle and Keigwin, 1987; Oppo and Fairbanks, 1987; Curry et al., 1988; Duplessy et al., 1988; Venz et al., 1999; Curry and Oppo, 2005; Marchitto and Broecker, 2006). During these periods the NADW production shifted to a shallower mode, in which Glacial North Atlantic intermediate water (GNAIW) was generated. The reduction of the AMOC decreased the amount of heat supplied to high latitudes allowing sea ice to cover most of the NGS and Labrador Sea areas and preventing open ocean convection.

Surface water characteristics of the subpolar North Atlantic are particularly important because changes in North Atlantic deep water ventilation and in the strength of the thermohaline circulation are driven by temperature and salinity of the subpolar North Atlantic surface waters (Broecker and Denton, 1989). Nevertheless, less attention has been paid to changes in the subpolar surface circulation compared those

---

* Corresponding author at: College of Marine Science, University of South Florida, 140 7th Avenue South, St. Petersburg, FL, 33701, United States. Tel.: +1 727 553 1002.
E-mail addresses: montsealonso82@gmail.com, montseag@usal.es, montserrat@mail.usf.edu (M. Alonso-Garcia).

0031-0182/$ – see front matter © 2011 Elsevier B.V. All rights reserved.
doi:10.1016/j.palaeo.2011.09.004

changes that happened in the deep water. Planktic foraminifers are a very valuable proxy to study the characteristics of surface water masses (Pflaumann et al., 2003; Kucera et al., 2005). In fact, in the NGS planktic foraminifer abundances have been used as a proxy not only for surface water temperature and salinity but also for sea ice coverage (Johannessen et al., 1994). At present, three surface water masses can be distinguished in the NGS (Fig. 1): Polar, Arctic and Atlantic waters (Swift and Aagaard, 1981; Swift, 1986). The Polar water is located in the western part of the NGS, and it is a cold and low salinity water mass mainly influenced by the East Greenland current (EGC). The Polar water is separated from the cold but higher salinity Arctic water by the Polar front (PF). The PF is close to the summer sea ice edge, thus the Polar water is perennially covered by sea ice. The Arctic front (AF) is the boundary between the Arctic water and the warm and high salinity Atlantic water (Helland-Hansen and Nansen, 1909; Dietrich, 1969; Swift and Aagaard, 1981). Since the maximum sea ice edge is slightly west of the AF, Arctic waters are seasonally covered by ice which promotes winter convection due to ice formation, and, in turn, lead to NGS deep water formation (Swift, 1986; Tomczak and Godfrey, 1994). Planktic foraminifer assemblages show clear differences between (1) the Polar water, in which *Neogloboquadrina pachyderma* sinistral (sin) is the most abundant species but planktic foraminifer flux is low; (2) the Arctic water, in which the planktic foraminifer flux is high and *N. pachyderma* sin is still the most abundant species; and (3) the Atlantic water, in which the planktic foraminifer flux is high and transitional to subpolar species such as *Neogloboquadrina pachyderma* dextral (dex), *Turborotalita quinqueloba* and *Globigerina bulloides* are the most abundant species (Johannessen et al., 1994). Additionally, the position of the AF is characterised by the boundary between high percentages of *N. pachyderma* sin and high percentages of *T. quinqueloba*, which is very abundant east of the AF.

Several authors have used planktic foraminifer species abundances as a proxy to infer the Polar and Arctic front positions for different Pleistocene intervals (Fronval et al., 1998; Wright and Flower, 2002; St. John et al., 2004). In this work, we analysed a high resolution record of planktic foraminifer assemblages from the subpolar North Atlantic Site U1314 in order to infer the evolution of surface water characteristics over four climatic cycles during the Mid-Pleistocene (ca. 800–400 ka) and its relationship to the AMOC. We took advantage of the location of the Integrated Ocean Drilling Program (IODP) Site U1314 in the subpolar gyre and compared our results with published data from other North Atlantic sites to reconstruct the approximate extent of winter sea ice coverage and AF migrations over the glacial–interglacial cycles. The increase in winter sea ice coverage is considered a key point inducing rapid climate changes in the continents, extremely decreasing winter temperatures and strengthening seasonality (Ruddiman and McIntyre, 1981; Isarin et al., 1998; Denton et al., 2005; Denton et al., 2010). Additionally, winter sea ice coverage plays a major role promoting ice sheet growth and decay (Gildor and Tziperman, 2001). Therefore, the knowledge of the distribution of surface water masses and winter sea ice coverage in the Northern North Atlantic over glacial–interglacial cycles is essential for a better understanding of climate development.

2. Regional setting

IODP Site U1314 was drilled in southern Gardar drift, south of Iceland (56° 21.8′ N, 27° 53.3′ W) at 2820 m water depth (Fig. 1). This site is located inside the subpolar gyre, currently influenced by the NAC which flows northeastwards across the North Atlantic into the Nordic Seas (Fig. 1). The NAC flows between the subtropical and subpolar gyres

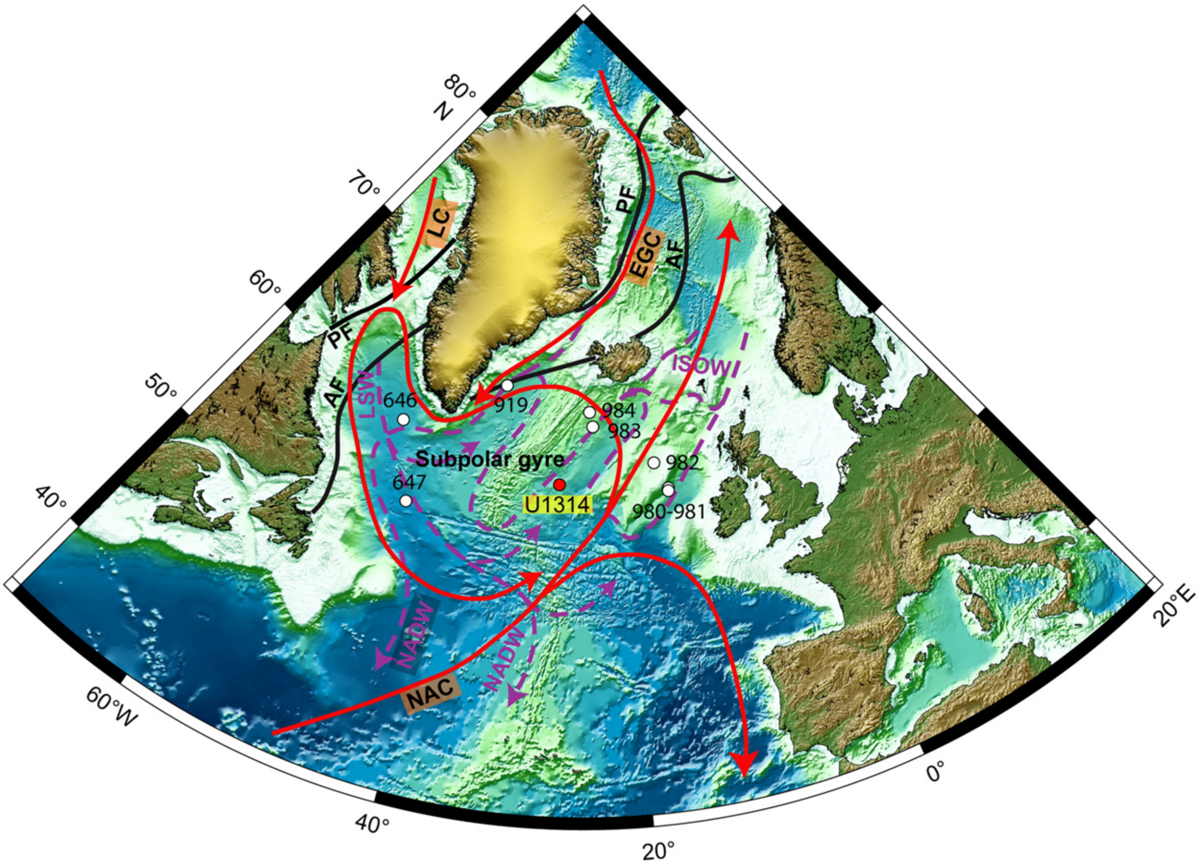

Fig. 1. Location of the IODP Site U1314 and other north Atlantic sites used to reconstruct the Arctic Front position. Red arrows represent main surface currents according to Schmitz and McCartney (1993). Present location of the Arctic and Polar fronts (AF and PF) is depicted according to Swift (1986). Purple dashed arrows represent deep ocean circulation after Dickson et al. (1990). EGC: East Greenland Current; NC: Norwegian Current; LC: Labrador Current; NAC: North Atlantic Current; DSOW: Denmark Strait Overflow water; ISOW: Iceland Scotland Overflow water; LSW: Labrador Sea water; NADW: North Atlantic Deep water. The map was provided by Integrated Ocean Drilling Program (IODP).

drawing water from them (Hansen and Østerhus, 2000), and near Iceland, the Irminger current (IC) splits from the NAC and flows towards the Greenland coasts mixing with the cold EGC. The EGC flows following East Greenland coast towards the Labrador Sea where it mixes with the Labrador current and together flow towards the NAC completing the gyre (Tomczak and Godfrey, 1994; Hansen and Østerhus, 2000). At present, the subpolar gyre water is highly influenced by the warm and high salinity water of the NAC because open ocean convection occurs in the Labrador Sea (Schmitz and McCartney, 1993). However, model simulations and oceanic observations suggest that a higher sea ice export through the EGC may change the characteristics of subpolar gyre water masses reducing convection in the Labrador Sea and causing the expansion of winter sea ice (Hakkinen and Rhines, 2004; Hatun et al., 2005; Born et al., 2009; Born et al., 2010). The characteristics of Polar, Arctic and Atlantic waters are well known for the modern NGS (Helland-Hansen and Nansen, 1909; Dietrich, 1969; Swift and Aagaard, 1981; Swift, 1986). Therefore, according to these characteristics we can track past changes in the extent of winter and summer sea ice in the subpolar North Atlantic by tracking the expansion of Polar and Arctic waters.

Site U1314 is also located in the path of the Iceland-Scotland Overflow water (ISOW), which is an important source of NADW (Fig. 1) and the sediments at this site reflect the strength of deep water formation in the NGS (Bianchi and McCave, 2000). Since the NAC is the main source of heat and moisture for high latitudes, the strength of the AMOC is closely linked to the subpolar surface water conditions. The results obtained in this work compliments the deep water circulation analysis showed in Alonso-Garcia et al. (2011) and helps to understand the oceanographic and climatic development of glacial–interterglacial cycles during the mid-Pleistocene. The features observed at these climatic cycles may also apply to those of the Late Pleistocene.

3. Materials and methods

Sediments at Site U1314 mainly consist of calcareous nannofossils and clay with minor and varying proportions of foraminifers, ice rafted debris (IRD), diatoms and radiolarians (Channell et al., 2006). Generally well preserved planktic foraminifers are the dominant component in the sand fraction, with lower proportions of benthic foraminifers, ostracodes, siliceous microfossils and IRD. The high sedimentation rate of the Gardar drift makes this site suitable for a high resolution study of glacial–interglacial climate shifts.

3.1. Chronological framework

The age model for the studied interval (Alonso-Garcia et al., 2011) was performed correlating the benthic δ^{18}O record of Site U1314 with the global benthic δ^{18}O stack of Lisiecki and Raymo (2005, hereafter LR04). The interval studied in this work, between 32.80 and 59.98 mcd (meters of composite depth), encompasses from ca. 400 to 800 ka. The mean sedimentation rate of the interval is 7.31 cm/ka which is similar to the rate described from preliminary data of Expedition 306 (Channell et al., 2006). The studied period is involved in the so-called Mid-Pleistocene transition (MPT), when climatic cyclicity shifted from the ~41 kyr-dominated cycles of the Early Pleistocene to the ~100 kyr-dominated cycles of the Late Pleistocene (Imbrie et al., 1993; Berger and Jansen, 1994; Mudelsee and Stattegger, 1997). This shift in the length of glacial–interglacial cycles was associated first with a gradual increase in the ice volume accumulation and severity of glacial periods (Mudelsee and Schulz, 1997; Mudelsee and Stattegger, 1997) and subsequently with the occurrence of extreme interglacial conditions after MIS 12 (Jansen et al., 1986; Berger and Wefer, 2003; Tzedakis et al., 2009). The transition to the "~100 kyr world" is unrelated to changes in the insolation forcing (Pisias and Moore, 1981) and although the processes and mechanisms that drove the MPT are still under debate (see review in Clark et al., 2006), several authors argue in favour of changes in the internal dynamics of the climate system as the trigger for this long-term cooling (Oerlemans, 1984; Mudelsee and Stattegger, 1997; Raymo et al., 1997; Paillard, 1998; Tziperman and Gildor, 2003; Rial, 2004; Maslin and Ridgwell, 2005), often associated with a decrease in atmospheric CO_2 (Mudelsee and Schulz, 1997; Raymo et al., 1997; Paillard, 1998). In regard to global ice volume, the 4 climatic cycles studied in this work recorded the presence of large ice sheets (Lisiecki and Raymo, 2005), particularly at MIS 16 and 12, which presented similar or even larger ice sheets than in the last 4 glacial cycles. However, interglacial conditions appear to have been colder than in the last 4 interglacial periods (Tzedakis et al., 2009), with slightly higher global ice volume (Lisiecki and Raymo, 2005) and lower atmospheric greenhouse gasses concentrations (Siegenthaler et al., 2005; Loulergue et al., 2008; Luthi et al., 2008).

3.2. Planktic foraminifer census counts

Planktic foraminifer assemblages were studied every 8 cm, which according to the age model represents an average resolution of 1094 years. Each sample was washed with deionized water through a 63 μm mesh to eliminate clay and other fine-grained particles. Then, samples were dry-sieved through a 150 μm mesh to separate two fractions, 63–150 μm and over 150 μm. Census counts were performed on the coarser fraction. Each sample was split multiple times until there were roughly 400 planktic foraminifer specimens (300 minimum). Relative abundances of the species found and specimens per gram of dry sediment were calculated using the census counts. Additionally, we calculated the fluxes of the different species using the dry density of the sediment (available at the IODP website http://iodp.tamu.edu/janusweb/general/dbtable.cgi?leg=306&site=1314).

A Q-mode factor analysis (Imbrie, 1963) with varimax rotation was performed on the downcore assemblages to reduce the variables and look for relationships between the different species found. Moreover, a mean annual sea surface temperature (SST) record was determined using planktic foraminifer assemblages. The SST record was calculated using a transfer function based on a back propagating artificial neural network (ANN) (Malmgren et al., 2001) trained on the MARGO (Multiproxy Approach for the Reconstruction of the Glacial Ocean surface) North Atlantic dataset (Kucera et al., 2005).

3.3. Benthic oxygen and carbon isotopes

The δ^{18}O and δ^{13}C records were mainly derived from the benthic foraminifer *Cibicidoides wuellerstorfi*, although during a few short intervals other *Cibicidoides* or even *Melonis pompilioides* were used due to the lack of *C. wuellerstorfi* (Alonso-Garcia et al., 2011). The analyses were performed on an automated carbonate preparation Kiel device I (prototype) coupled to a Finnigan MAT 251 mass spectrometer at the Leibniz laboratory for radiometric dating and Isotope research, in the University of Kiel. Analytical precision based on international standards NBS-19 and NBS-20 was better than 0.07‰ for δ^{18}O and better than 0.05‰ for δ^{13}C. Results are reported on the Vienna Pee Dee Belemnite (VPDB) standard scale (Coplen, 1996).

4. Results

4.1. Planktic foraminifer assemblages

Despite the fact that 16 planktic foraminifer species were identified, only five of them present abundances high enough to be considered as important indicators of surface water masses conditions. Those species are *N. pachyderma* sin, *N. pachyderma* dex, *Globorotalia inflata*, *G. bulloides* and *T. quinqueloba* (Fig. 2).

Census counts reveal two clear groups of fauna. During glacial stages diversity was very low and the assemblage was almost monospecific, dominated by the species *N. pachyderma* sin, accompanied by variable amounts of *T. quinqueloba* and low percentages of *N. pachyderma* dex, *G. inflata* and *G. bulloides* (Fig. 2). *N. pachyderma* sin shows sharp changes in relative abundance, with percentages between 65 and 98% during glacial periods and percentages below 15%, even reaching values of about 1%, during interglacial periods. This species typically thrives in polar environments at temperatures between −1 and 8 °C (Tolderlund and Bé, 1971; Bé, 1977; Bauch et al., 1997; Pflaumann et al., 2003) and it is particularly abundant in the Arctic water (Johannessen et al., 1994). On the other hand, during interglacial periods, more diversified microfauna was found (Fig. 2) and three species were the main components of the assemblage, *N. pachyderma* dex, *G. inflata* and *G. bulloides*. These 3 species were commonly accompanied by variable amounts of *T. quinqueloba*, and little amounts of other species (see later in this section). *N. pachyderma* dex, *G. inflata* and *G. bulloides* reached relative abundances up to 60–70%, 30–40% and 20–40%, respectively, during the interglacial periods whereas during glacial times *N. pachyderma* dex abundance was about 5%, *G. bulloides* below 5% and *G. inflata* near zero. *N. pachyderma* dex and *G. bulloides* live in subpolar environments preferably between 10 and 18 °C (Tolderlund and Bé, 1971; Bé, 1977; Reynolds and Thunell, 1985; Hemleben et al., 1989) whereas *G. inflata* is a transitional species that lives in a wide temperature range, but preferably between 10 and 20 °C (Bé and Tolderlund, 1971). These three species account for the major part of the transitional-subpolar assemblage found in the NAC water.

T. quinqueloba presented higher abundances at certain intervals either during glacial or interglacial periods, ranging between approximately 0 and 50% (Fig. 2). This species thrives nowadays in periods of high phytoplankton productivity when the mixed layer is deep (Stangeew, 2001; Simstich et al., 2003). Johannessen et al. (1994) reported the maximum abundance of *T. quinqueloba* in the Nordic Seas just east of the Arctic front covering the thermal gradient between the Arctic waters and the Atlantic waters.

Among the less abundant species *Globigerinita glutinata* and *Globorotalia scitula* were recorded in percentages below 20 and 10% respectively. Besides, many subtropical species like *Globorotalia truncatulinoides*, *Neogloboquadrina dutertrei*, *Orbulina universa*, *Globigerinoides ruber* white, *Globorotalia crassaformis*, *Globorotalia hirsuta* and *Beella digitata* were found below 2% altogether (Fig. 2).

Preservation in the studied interval was analysed regarding at the planktic foraminifer fragmentation index, which represents in percentage

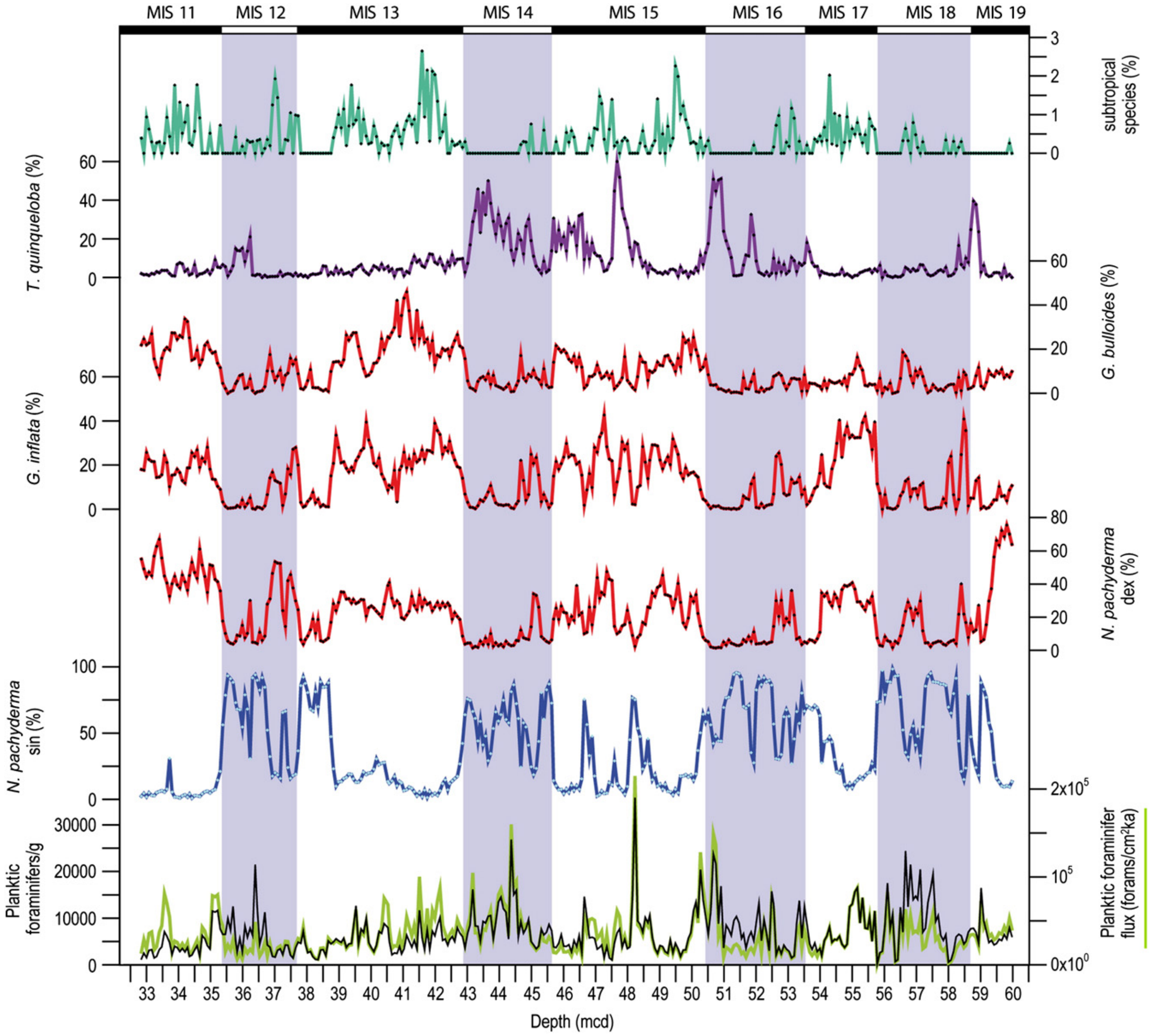

Fig. 2. Planktic foraminifer assemblage of Site U1314 (only the most relevant species are shown). From top to bottom: subtropical species, *T. quinqueloba*, *G. bulloides G. inflata*, *N. pachyderma* dex and *N. pachyderma* sin. At the bottom of the graph planktic foraminifers per gram of dry sediment (black line) and planktic foraminifer flux (green line) are depicted. Marine isotope stages (MIS) are shown at the top and the glacial intervals are highlighted with vertical violet bars.

Table 1
Factor scores obtained from the planktic foraminifer factor analysis. The highest factor scores are highlighted in grey indicating which species are important in each factor. The variance explained by each factor is shown at the bottom.

Species	Factor scores		
	Factor 1	Factor 2	Factor 3
O. universa	−0.627	−0.340	−0.372
G. ruber (w)	−0.703	−0.313	−0.410
G. siphonifera	−0.688	−0.314	−0.402
G. bulloides	1.366	−0.321	0.311
B. digitata	−0.758	−0.301	−0.397
T. quinqueloba	−0.436	0.049	3.343
N. pachyderma (s)	−0.202	3.387	−0.195
N. dutertrei	−0.737	−0.291	−0.431
N. pachyderma (d)	1.935	0.382	−0.652
G. inflata	1.775	−0.561	0.245
G. truncatulinoides	−0.687	−0.330	−0.421
G. crassaformis	−0.626	−0.351	−0.422
G. scitula	−0.350	−0.348	0.004
G. glutinata	0.738	−0.349	−0.203
Explained variance (%)	49.071	37.346	9.631

the amount of fragments respect to the total amount of foraminifers plus fragments (Thunell, 1976). The fragmentation index is generally lower than 20%, indicating very good preservation in the samples, except for some short intervals where dissolution increased but the index hardly reached 40%. Miao et al. (1994) described in samples from the China Sea that the assemblages began to suffer modifications due to dissolution when the 40% of fragmentation was exceeded. Therefore, we can assume that the assemblages presented here are not modified by dissolution and they are a suitable proxy for inferring water masses characteristics.

4.3. Factor analysis of planktic foraminifer assemblages

Although two groups of microfauna can be easily distinguished, planktic foraminifer relative abundances were reduced using factor analysis. We found that 96% of the variance was explained by the first three factors (see Table 1 for the explained variance of each factor). We rejected the fourth factor and followings because the variance explained by them was lower than 5%. Species scores for the three factors are listed in Table 1. Factor loadings are depicted in Fig. 3 and the actual values are available in supplementary data (Appendix A). In Factor 1, which explained 49.07% of the variance, the highest factor scores were found in transitional-subpolar water species (*N. pachyderma* dex, *G. inflata* and *G. bulloides*, see Table 1). Factor 2, which explained 37.34% of the variance, was only related to the polar species *N. pachyderma* sin. In the third Factor, which explained 9.64% of the variance, only *T. quinqueloba* presented high factor scores. Factor loadings of Factors 1 and 2 are generally opposite, however high factor loadings of Factor 3 co-occurred with medium-high values of Factor 1 or 2 indistinctly (see Fig. 1 and Appendix A).

5. Discussion

5.1. Interpretation of the factor analysis

Since Factor 1 is related to the transitional-subpolar water species, we suggest that this factor indicates the presence of the temperate waters of the NAC where these species thrive at present in the subpolar North Atlantic (Bé and Tolderlund, 1971; Tolderlund and Bé, 1971; Bé, 1977; Reynolds and Thunell, 1985; Hemleben et al., 1989). A similar conclusion was obtained for Factor 2, attributed to the cold and low salinity waters in which *N. pachyderma* sin thrives at present (Tolderlund and Bé, 1971; Bé, 1977; Reynolds and Thunell, 1985; Hemleben et al., 1989; Stangeew, 2001; Simstich et al., 2003). Therefore, the glacial assemblage is associated with Factor 2 and the interglacial assemblage with Factor 1. There is a strong parallelism between the abundance of *N. pachyderma* sin and loadings of Factor 2 and between the abundance of the transitional-subpolar species and loadings of Factor 1 (Fig. 3). Both the factor loadings and the relative abundances show abrupt changes, within ~3000 years or even less. These abrupt shifts indicate

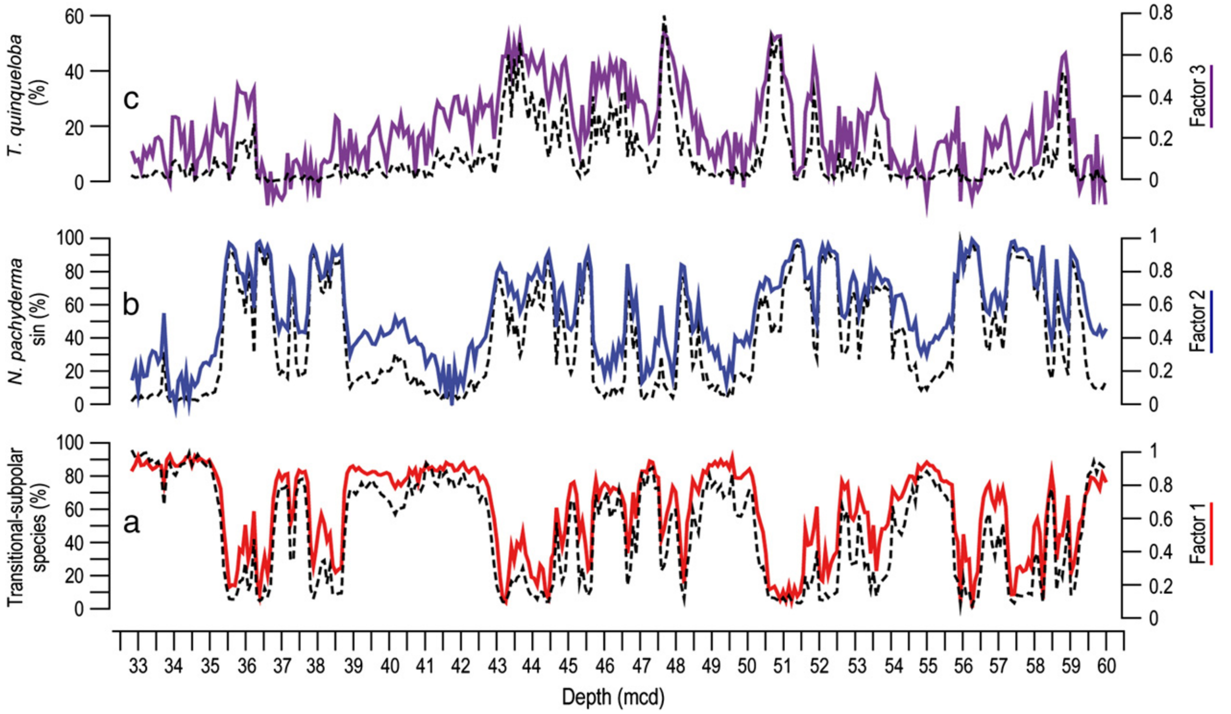

Fig. 3. Comparison between factor loadings and the abundance of the most important species of each factor. a) Factor 1 (red line) and the subpolar species (*N. pachyderma* dex + *G. inflata* + *G. bulloides*) relative abundance (black dashed line); b) Factor 2 (blue line) and the polar species *N. pachyderma* sin relative abundance (black dashed line); and c) Factor 3 (purple line) and *T. quinqueloba* relative abundance (black dashed line).

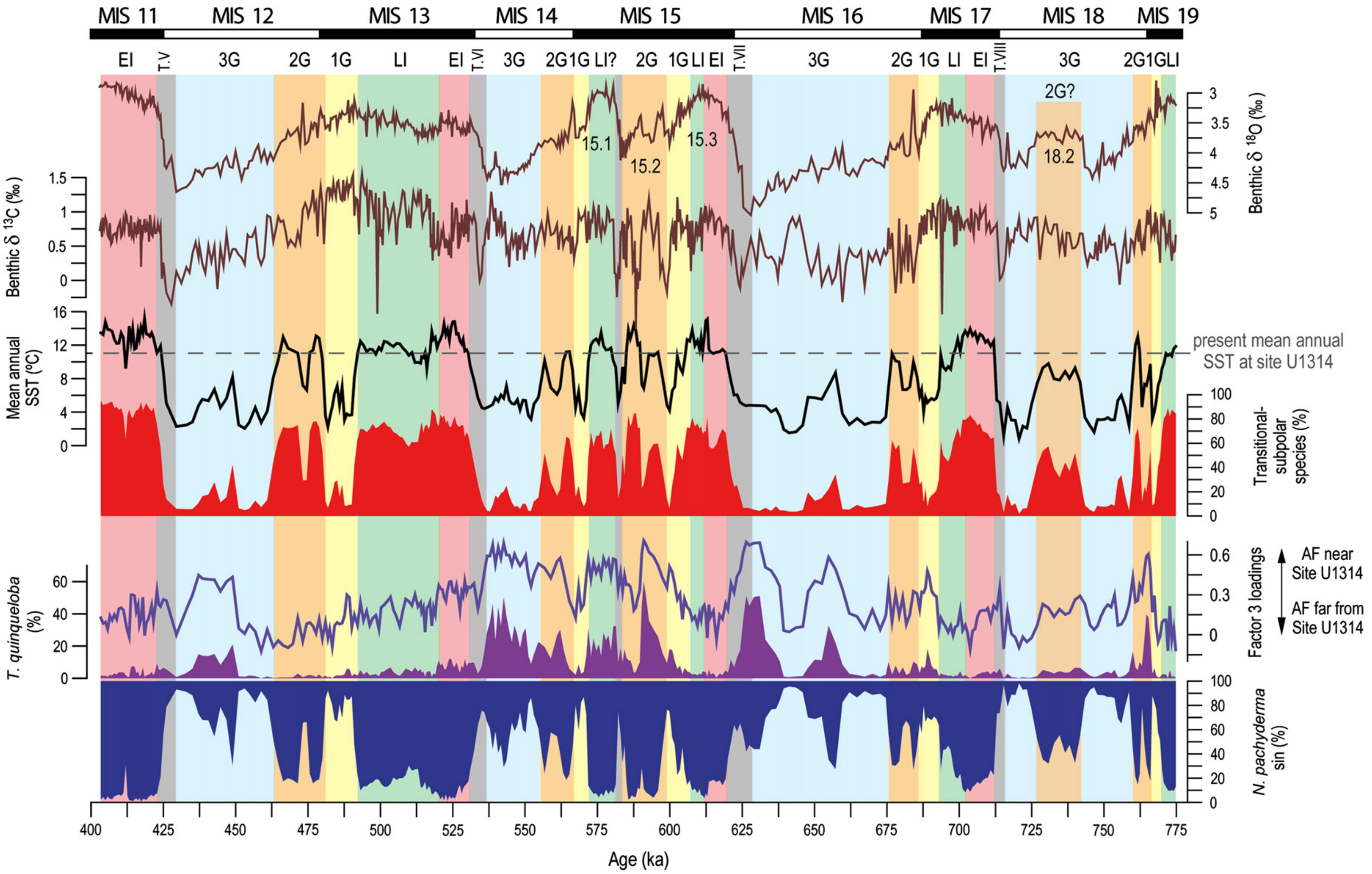

Fig. 4. Different phases of development of climatic cycles based on AF migrations: early interglacial phase (EI, vertical red bars), late interglacial phase (LI, vertical green bars), first phase of glacial periods (1 G, vertical yellow bars), second phase of glacial periods (2 G, vertical orange bars) and third phase of glacial periods (3 G, vertical blue bars). From top to bottom: benthic δ^{18}O record (Alonso-Garcia et al., 2011); benthic δ^{13}C record (Alonso-Garcia et al., 2011); mean annual sea surface temperatures (Alonso-Garcia et al., 2011); transitional-subpolar species (*N. pachyderma* dex + *G. inflata* + *G. bulloides*) relative abundances; Factor 3 loadings; *T. quinqueloba* relative abundances; and *N. pachyderma* sin relative abundances. Fill colour of *N. pachyderma* sin is inverted in order to better appreciate the coupling with *T. quinqueloba* when the Arctic front is near Site U1314. Terminations are shown with vertical grey bars and labelled from V to VIII. Marine isotope stages (MIS) are shown at the top and the substages mentioned in the article are indicated below the benthic δ^{18}O record.

a) Early interglacial phase

b) Late interglacial phase

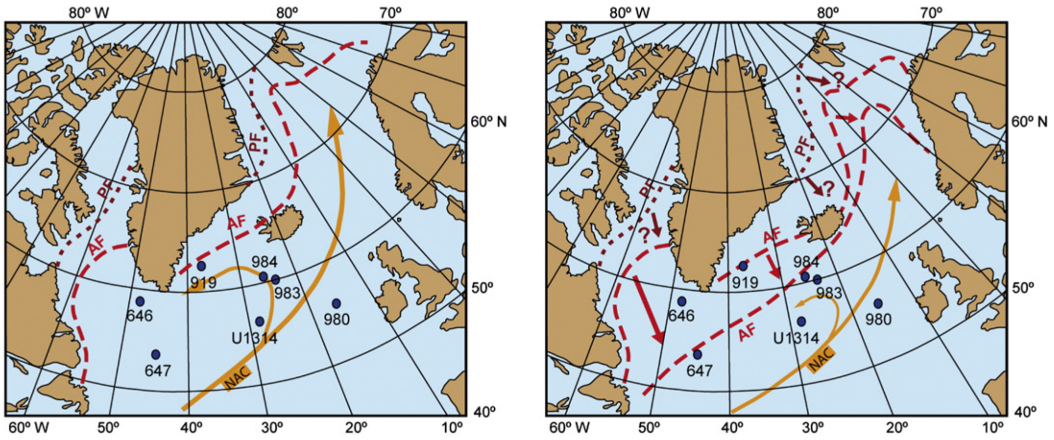

c) First phase of glacial periods

d) Second phase of glacial periods

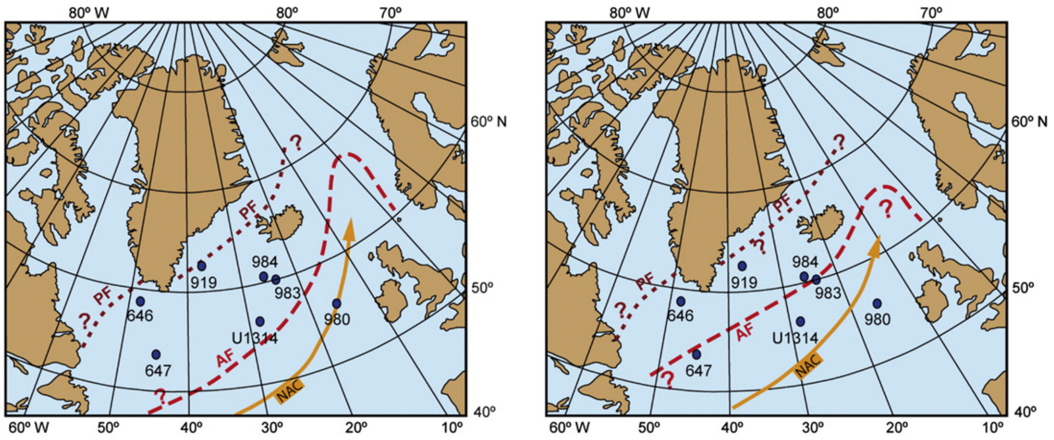

e) Third phase of glacial periods

f) Terminations

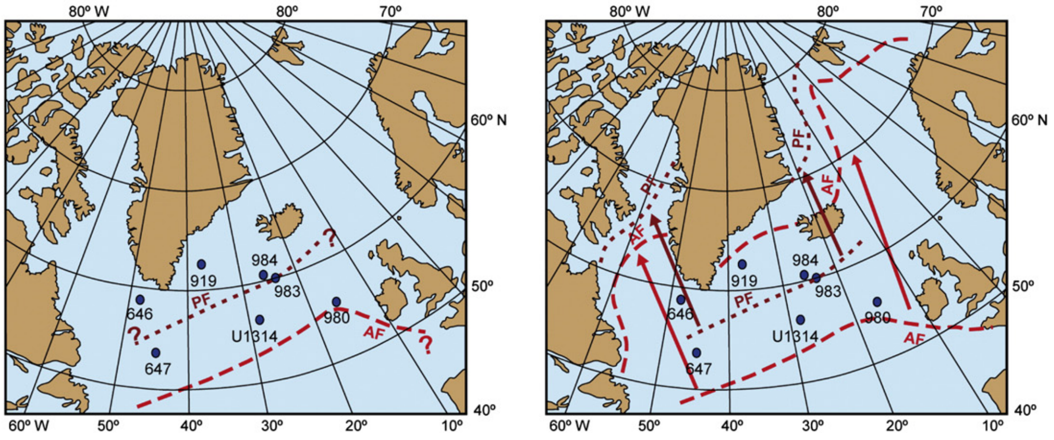

Fig. 5. Inferred position of the Arctic and Polar fronts and surface circulation in the North Atlantic for each phase of climatic cycles.

that the glacial assemblage was rapidly replaced by the interglacial assemblage (or vice versa) due to rapid changes in the subpolar surface water conditions. In other words, the extent of the Arctic waters changed rapidly and so the planktic assemblage did.

The high factor scores of *T. quinqueloba* in Factor 3 suggest that this factor is indicating the presence of the AF near the site (Johannessen et al., 1994). The loadings of Factor 3 are similar to the relative abundance of *T. quinqueloba* (Fig. 3) but in the loadings many peaks are magnified. We reckon that the analysis of Factor 3 shifts is more helpful to evaluate AF migrations than the mere abundance of *T. quinqueloba*. The fact that high values of the loadings of Factor 3 (Fig. 3) are often coeval with medium-high values of Factor 1 loadings (or Factor 2 loadings) may reflect that the AF was near the site but the NAC (or the Arctic waters) mainly influenced the studied area. Thus, when analysing the AF shifts we also pay attention to the loadings of Factors 1 and 2 and to the species relative abundances.

The numerous shifts in the values of Factor 3 loadings suggest that the AF was not exactly in the same location during all glacial (or interglacial) periods but its location was variable. The factor analysis combined with planktic foraminifer relative abundances allowed us to reconstruct surface water masses affinity to NAC, AF and Arctic waters over glacial–interglacial cycles at Site U1314.

5.2. Arctic front position over glacial–interglacial cycles

Interglacial cycles at Site U1314 began with low relative abundance of *N. pachyderma* sin, below 20%, which usually shows a decreasing trend until values below 10% (Figs. 2 and 4), whereas the transitional-subpolar species presented high values, above 65% (Fig. 4). *T. quinqueloba* relative abundance was lower than 10% (Figs. 2 and 4) at the beginning of interglacial periods and presented a decreasing trend as well as *N. pachyderma* sin abundance. Planktic foraminifer assemblages found at Site U1314 at the beginning of interglacial periods were similar to present assemblages at this site, according to the planktic foraminifer dataset of MARGO (Kucera et al., 2005), and suggest that the AF was further north of Site U1314. Although *N. pachyderma* sin thrives in different seasons at different areas of the North Atlantic (Fraile et al., 2009), this species commonly lives below the thermocline and pycnocline (Tolderlund and Bé, 1971; Bé, 1977; Carstens and Wefer, 1992; Bauch et al., 1997; Stangeew, 2001; Simstich et al., 2003; Nyland et al., 2006; Jonkers et al., 2010) reflecting the temperature of the winter mixed-layer water mass and, hence, it can be used as a winter proxy. The decrease in *N. pachyderma* sin and *T. quinqueloba* percentages may suggest that winter conditions gradually became warmer at Site U1314. The increasing mean annual SST (Fig. 4) could also indicate that winter temperatures became milder. Similar trends and relative abundances of *N. pachyderma* sin were also found at Site ODP 980 (Wright and Flower, 2002) with values below 15% except during MIS 17 when relative abundance was around 25%. Additionally, at Sites ODP 984 (Wright and Flower, 2002), 647 and 646 (Aksu et al., 1989; Aksu et al., 1992) lower abundances of *N. pachyderma* sin were recorded respect to the glacial periods although higher than in Sites U1314 and 980. Moreover, the high diatom recovery at ODP Sites 983 and 919 (Koç and Flower, 1998; Koç et al., 1999) suggest that the polar water was further north of both sites. Based on all these data, we suggest that during early interglacial periods the average position of the Polar and Arctic fronts was similar to their present location or even northwards (Fig. 5a), and surface water conditions in the subpolar North Atlantic were warm.

During the second part of the interglacial periods the relative abundances of *N. pachyderma* sin and/or *T. quinqueloba* slightly increased at Site U1314 (Fig. 4). The transitional-subpolar species and the mean annual SST slightly decreased suggesting that although the assemblage was predominantly transitional-subpolar, mean annual conditions started to cool indicating the return of colder winters. At Site 980, there was also a small increase in *N. pachyderma* sin and *T. quinqueloba* relative abundances (Wright and Flower, 2002), whereas at Sites 984, 647 and 646 *N. pachyderma* sin increased towards very high values above 85% at Site 984 (Aksu et al., 1989; Aksu et al., 1992; Wright and Flower, 2002). The winter cooling trend suggests that the AF may have shifted slightly southwards close to sites 984 and 647 (Fig. 5b).

The inflection in the benthic δ^{18}O record towards higher values at MIS 13/12, 15.1/14, 15.3/15.2 and 17/16 indicates that the ice volume started to increase towards a new glacial period (Fig. 4). During glacial initiations *N. pachyderma* sin increased rapidly, reaching glacial values (above 65%) in a few thousands of years. *T. quinqueloba* usually shows a subtle increase but the loadings of Factor 3 show a stronger increase which suggests the proximity of the AF. The high relative abundance of *N. pachyderma* sin at sites west and north of Site U1314 indicate that the Arctic waters influenced the western subpolar North Atlantic (Aksu et al., 1989; Aksu et al., 1992; Wright and Flower, 2002) whereas at Site 980 the assemblage was still predominantly transitional-subpolar. This suggests that sea surface temperatures drop considerably at the western subpolar North Atlantic but not in the eastern part. According to these results, during glacial initiations the AF underwent a rapid southeastward shift (Fig. 5c) which resulted in a strong east–west SST contrast in the subpolar North Atlantic, similar to the contrast observed at present in the NGS where the warm water of the NAC is east of the AF (in the Norwegian Sea) and the Arctic waters are west of the AF (in the Greenland Sea). Planktic foraminifer and diatom data from Sites 646 and 919 suggest the absence of perennial sea ice at these sites during the beginning of glacial periods (Aksu et al., 1992; Koç and Flower, 1998) and, therefore, the sites were south of the PF (Fig. 5c).

At Site U1314 the first significant ice-rafting event of each glacial period was linked to an abrupt SST shift (Alonso-Garcia et al., 2011) which marks the onset of the second phase of glacial periods (Fig. 4). Although the assemblage was predominantly transitional-subpolar and SST reached interglacial values during the warmest intervals, this phase is characterised by rapid SST changes linked to ice-rafting events (Alonso-Garcia et al., 2011). These warmest intervals occurred after the ice-rafting event and lasted 2–5 kyr. At Site 980 sea surface conditions were similar to the first phase of glacial periods or slightly warmer after ice-rafting events (Wright and Flower, 2002) whereas at Sites 984 and 647 the subpolar assemblage increased (Aksu et al., 1989; Wright and Flower, 2002) but SST were less warm than at Site U1314. During this phase the AF was north of Site U1314 but probably close to Sites 647 and 984 whereas the PF was probably north of Sites 919 and 646 (Fig. 5d).

After the second warm event there was a rapid return to the dominance of the glacial assemblage. At Site U1314 the relative abundance

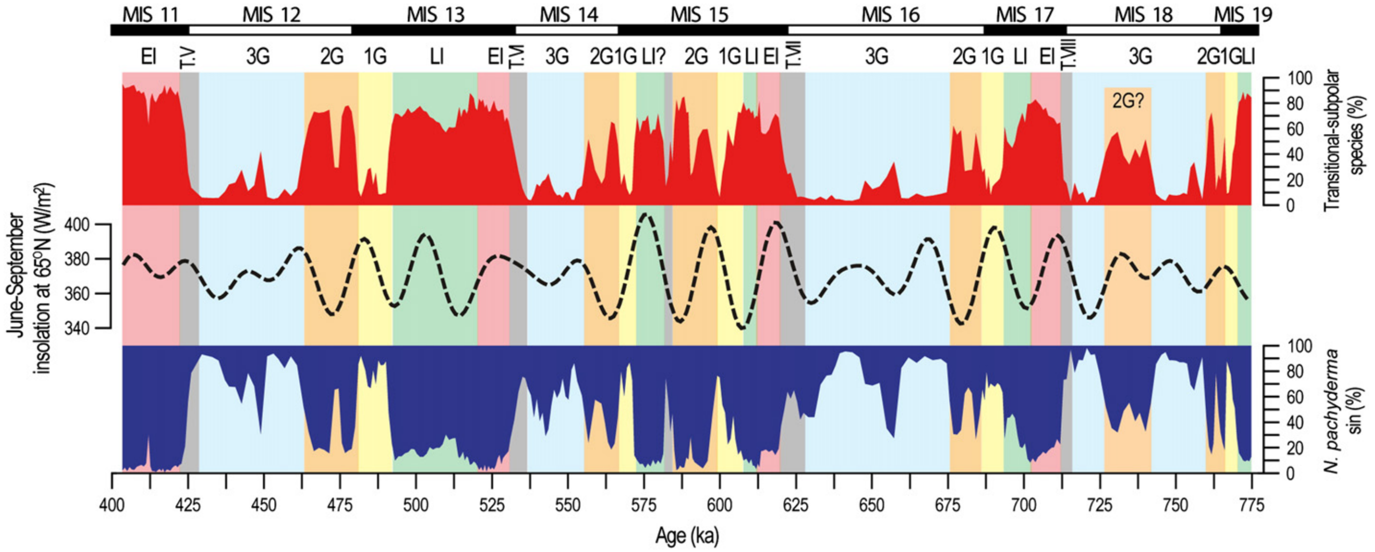

Fig. 6. Comparison between the planktic foraminifer assemblages and insolation at 65°N and its relationship with the different phases determined for the climatic cycles.

of the transitional-subpolar assemblage was lower than 35% and reached values below 5% during the coldest intervals (Fig. 4). At Site 980 *N. pachyderma* sin significantly increased and for the first time in each climatic cycle reached values above 80% (Wright and Flower, 2002). The sites northwest of Site U1314 were also dominated by polar assemblages (Aksu et al., 1989; Aksu et al., 1992; Wright and Flower, 2002) suggesting that during the third phase of glacial periods the AF was located almost east–west from Newfoundland to Ireland and all the subpolar North Atlantic was characterised by very low SST (Fig. 5e). The diatom records of Sites 983 and 919 suggested that sea ice perennially covered these areas during most of the glacial period (Koç and Flower, 1998; Koç et al., 1999) and, hence the PF was probably located southwards of these sites (Fig. 5e). In Site U1314 planktic foraminifer fluxes (Fig. 2) were high during all glacial periods indicating that sea ice cover was only seasonal and, therefore the PF was always north of Site U1314. During this phase several ice-rafting events occurred, but the warming events linked to them were less warm than those of the second phase of glacial periods. The warming events of the third phase were characterised by small increases in the transitional-subpolar species and large increases in *T. quinqueloba* at Site U1314 (Fig. 4) and also at Site 980 (Wright and Flower, 2002).

During Terminations the assemblages underwent a strong change from the dominance of *N. pachyderma* sin to the dominance of the transitional-subpolar species in a few thousand years. Both the Arctic and Polar fronts migrated northwestwards very fast reaching the early interglacial position in a very short period of time.

5.3. Division of climatic cycles

Although there is a wide diversity among glacial and interglacial periods and each climatic cycle presents several inherent features, we found that, according to the sea surface conditions, each climatic cycle from 800 to 400 ka can be divided in 5 phases of development plus the Terminations. Moreover, the different sea surface conditions features of each phase were associated with a characteristic state in ice volume and deep water circulation.

Early interglacial phase (vertical red bars in Figs. 4 and 6; Fig. 5a). After Terminations (grey bars) planktic foraminifer assemblages indicate that the AF was further north and NAC waters influenced most of the subpolar North Atlantic. The high North Atlantic benthic δ^{13}C values (e. g. Alonso-Garcia et al., 2011; Wright and Flower, 2002) suggest that deep water formation was active in the NGS. Furthermore, the warm temperatures in the subpolar gyre indicate a strong advection of NAC water via the IC and suggest that deep water formation in the Labrador Sea was also strong. The AF was close to its present position or perhaps even more northwestwards, keeping Arctic waters in the Greenland and Labrador Seas. It is likely that the PF was also in a similar position as at present.

Late interglacial phase (vertical green bars in Figs. 4 and 6; Fig. 5b). The small increases of *N. pachyderma* sin and *T. quinqueloba* relative abundances suggest that interglacial conditions began to cool probably due more severe winter temperatures which diminished the mean annual SST. During this phase benthic δ^{18}O shows that ice sheets were not growing (Fig. 4), in fact the δ^{18}O was stable or slightly decreasing. Although the ice sheets were not growing, the records from all the sites mentioned earlier suggest the AF progressively moved southeastwards. It appears that the early interglacial phase is related to high summer insolation at 65ºN whereas the late phase is related to the decrease of summer insolation (Fig. 6). The decrease in summer insolation at high latitudes may have favoured growth and persistence of sea ice in the Arctic Ocean and enhanced sea ice export through the EGC during winters, as modelled for the Eemian (Born et al., 2010). Consequently, ocean circulation in the Arctic and subpolar North Atlantic regions may have undergone a reorganization which reduced convection in the Labrador Sea. Additionally, the increasing amount of sea ice may have increased albedo and ocean isolation from the atmosphere, and as a consequence annual SST decreased at high latitudes (Crucifix and Loutre, 2002). A similar scenario with decreasing SST occurred during the late part of MIS 5e, when the northern North Atlantic cooled in response to a decrease in June insolation at 65°N, while the mid-latitudes were still warm (Cortijo et al., 1994; Fronval and Jansen, 1997; McManus et al., 2002; Tzedakis, 2005). In summary, during the late interglacial periods the surface waters of the subpolar gyre slightly cooled and freshened during winters. This reduced deep water formation in the Labrador Sea, and in turn weakened the advection of warm water to the subpolar gyre through the IC. Despite the lack of planktic foraminifer records at the NGS for the studied interval, we assume that the AF might have moved similarly to what was reported for late Eemian (Fronval et al., 1998) and that the enhanced sea ice export also expanded Arctic waters in the NGS, although deep water convection was hardly affected because convection in this area is less sensitive to the increase in sea ice export (Born et al., 2010).

However, the duration and characteristics of this phase are variable among the interglacial periods studied. The second phase of the interglacial period MIS 13 is outstandingly long. It encompasses almost two insolation minima and one maximum, although the insolation maximum was not associated with so high SST as during the first phase of interglacial periods. It is also remarkable that during all MIS 15.1 *N. pachyderma* sin and *T. quinqueloba* relative abundances were moderate; particularly *T. quinqueloba* relative abundance was about 20% and the Factor 3 loadings were also high (Fig. 4). This suggests that, after the small "Termination-like event" occurred at MIS 15.2/15.1, sea surface conditions were colder than after the other Terminations (T.V to VIII) and more similar to the second phase of the interglacial stages despite the insolation maximum (Fig. 6). In general, during interglacial periods the strength of summer insolation at 65ºN seems to be linked to sea surface conditions but it is not the only forcing controlling them, and when other factors appeared interglacial conditions can be modified like at MIS 13 or MIS 15.1. Assessing which factors modified interglacial conditions during these periods was not possible using only the datasets presented in this work, however more work should be done in this line to understand not only past interglacial climate forcings but also the present ones.

First phase of glacial periods (vertical yellow bars in Figs. 4 and 6; Fig. 5c). At glacial inceptions ice sheets started to grow and the presence of the polar fauna indicated that the AF shifted southeastwards, expanding the Arctic water in the central and western subpolar North Atlantic (Aksu et al., 1989; Aksu et al., 1992; this work), whereas in the eastern part the subpolar North Atlantic transitional assemblages indicate the presence of the warm water of the NAC (Wright and Flower, 2002). This "lagging warmth" at the beginning of glacial periods in the eastern North Atlantic was attributed to the persistence of the NADW formation in the NGS, as suggested by the high benthic δ^{13}C values (see Fig. 4, Alonso-Garcia et al., 2011; Wright and Flower, 2002), which maintained the NAC flow active and provided warmth to the eastern North Atlantic. This pattern has also been observed during other glacial initiations over the Late Pleistocene (Ruddiman and McIntyre, 1979; Ruddiman et al., 1980; Oppo et al., 2001; McManus et al., 2002; Oppo et al., 2006).

During glacial initiations insolation was usually low (Fig. 6) and that allowed sea ice to continue expanding and thickening in the western subpolar North Atlantic, which may have strongly reduced Labrador Sea convection. Although insolation was high during MIS 16 glacial initiation (Fig. 6), SST in the subpolar North Atlantic dropped indicating the expansion of Arctic waters in the subpolar gyre. Therefore, it would appear that sea ice began to expand due to low insolation in the late interglacial periods but afterwards other feedbacks amplified the sea ice expansion. The albedo produced by the sea ice has been suggested as one of the amplifiers for the initiation of the last glacial period, promoting ice sheet growth in North America and NW Europe (Crucifix and Loutre, 2002). Low summer insolation at high latitudes can promote the accumulation of snow in the continents, but as model simulations suggest that insolation is not enough to produce large ice sheet growth, and other feedbacks like albedo, atmospheric CO_2 drops and ocean circulation patterns must have been involved in the increase of ice volume at glacial initiations (Crucifix and Loutre, 2002; Wang and Mysak, 2002; Landais et al., 2006; Bonelli et al., 2009). The data presented in this work also suggests that once the sea ice expanded above a certain threshold (which we cannot quantify here) the SST in the western subpolar North Atlantic dropped rapidly triggering a new glacial period despite subsequent insolation rises.

During this phase the sea ice export to the subpolar gyre may have been stronger than in the late interglacial periods and deep water formation in the Labrador Sea may have been very much reduced. Therefore, if the NADW was mainly generated in the NGS it is likely that the volume of deep water production was significantly reduced weakening the AMOC to some extent, as it was suggested in Born et al. (2010) model. However, we cannot discard that intermediate water started to be generated at the western North Atlantic during this phase, as it was described during full glacial conditions (Boyle and Keigwin, 1982; Curry et al., 1988; Duplessy et al., 1988).

Second phase of glacial periods (vertical orange bars in Figs. 4 and 6; Fig. 5d). This phase is characterised by a return of the transitional-subpolar assemblages to the central North Atlantic and a northward shift of the AF to a position similar to the late interglacial phase although the ice volume was larger than during the previous phases. Additionally, the first significant ice-rafting events occurred and consequently the production of deep water in the NGS began to undergo reductions which led to the glacial circulation mode (Alonso-Garcia et al., 2011). The rapid warming events that followed the ice-rafting events may have been linked to the upwelling of the warm and salty water of the NAC which was stored in the subsurface layer due to the reduction of the AMOC during ice-rafting events (Moros et al., 2002; Rasmussen and Thomsen, 2004; Alonso-Garcia et al., 2011). The reason why the first two warming events that followed the first two significant ice-rafting events were much warmer than the subsequent ones is because prior to the iceberg calving the thermohaline circulation was strong. The dampening of the AMOC drove the storage of a huge amount of warm water in the North Atlantic which was upwelled as soon as the stratification produced by the ice-rafting was broken. This phase may be seen as a transition between the first and the third phase of glacial periods, in which deep ocean circulation changed from an active AMOC to a reduced AMOC, typical of full glacial conditions.

Third phase of glacial periods (vertical blue bars in Figs. 4 and 6; Fig. 5e). The sharp increase in *N. pachyderma* sin at mostly all the subpolar North Atlantic sites marks the onset of the full glacial conditions. During this phase the ice volume accumulated on the continents was large, deep water formation was curtailed in the NGS (Alonso-Garcia et al., 2011) and deep ocean circulation shifted to the glacial mode in which Glacial North Atlantic intermediate water was generated (Boyle and Keigwin, 1982; Curry et al., 1988; Duplessy et al., 1988). During the coldest intervals the AF was almost east–west and the PF was below Iceland. However, after the most significant ice-rafting events SST slightly increased and high percentages of *T. quinqueloba* at Sites U1314 and 980 suggest that the AF moved slightly northwards.

It is remarkable that MIS 15.2 represents a glacial period that never reached the third phase. Perhaps the reason why MIS 15.1 was colder than other interglacial periods is because the termination that preceded this interglacial was of low amplitude. Further research should be done to shed light on the development of MIS 15/14 climatic cycle. Additionally, the warm interval MIS 18.2 presents similar characteristics to the second phase of glacial periods, in which ice volume was lower than in the third phase and the SST warmer (Fig. 4). The occurrence of this warm period may also resemble the warming events of the third phase but with a longer duration and higher SST, therefore its classification is unclear. These two anomalous intervals represent a different pattern in the development of the climatic cycles that might be associated with the Mid-Pleistocene transition (Mudelsee and Schulz, 1997; Mudelsee and Stattegger, 1997).

Terminations (vertical grey bars in Figs. 4 and 6; Fig. 5f). During Terminations the AF moved northwestwards rather fast and subpolar-transitional assemblages settled in the subpolar North Atlantic in a few thousand years. The rapid migration of the AF and the rapid change from glacial to interglacial conditions has been a long-standing problem that is still not fully understood (Denton et al., 2010).

5.4. Long term changes in AF position?

Wright and Flower (2002) reported that the Arctic front position changed before and after MIS 16. Regarding at glacial periods, Site U1314 planktic foraminifer assemblages suggest that sea surface temperatures were slightly colder at MIS 18, and Site 980 and 984 also show slightly higher percentages of *N. pachyderma* sin in glacial periods 18, 20 and 22. Interglacial sea surface temperatures at Site U1314 were similar before and after MIS 16 although only the interglacial period MIS 17 is fully included in the studied interval. At Sites 980 and 984, MIS 17 shows higher *N. pachyderma* sin abundances, which indicates slightly colder conditions (Wright and Flower, 2002) but *N. pachyderma* sin abundances were very low during interglacial periods MIS 21 and 19. Site U1314 radiolarian census counts from MIS 31 to 19 (Hernández-Almeida et al., in press) show that after MIS 21 the warm-water radiolarian species increased, which points to a northward shift of the AF and the presence of the transitional-subpolar water in the area. Diatom and alkenone data from nearby sites also support colder surface water conditions before MIS 21 (McClymont et al., 2008; Shimada et al., 2008).

Therefore, new evidences suggest that for interglacial periods the AF gradually shifted northwards after MIS 21 linked to the oceanic and climatic changes that took place at ~900 ka. Whereas for glacial periods the AF might have shifted afterwards, probably after MIS 18, which was the last glacial period with very low temperatures at Sites 980 and U1314. It is likely that the AF migrated in two steps, first for interglacial periods and then for glacials, like the MPT oceanic and climatic changes which occurred in several steps (e.g. Mudelsee and Schulz, 1997; Clark et al., 2006). Unfortunately, the time interval studied in this work does not fully resolve this question and more data covering the entire MPT is necessary to clarify it.

6. Conclusions

Planktic foraminifer assemblages from the subpolar North Atlantic Site U1314 have been studied to analyse sea surface conditions from ca. 800–400 ka. Factor analysis of the planktic foraminifer assemblages shows that three factors controlled the assemblage. The first factor (which explained 49% of the variance) is dominated by the transitional-subpolar species *N. pachyderma* dex, *G. bulloides* and *G. inflata*, the second factor (37%) is dominated by the polar species *Neogloboquadrina pachyderma* sin and the third factor (9%) is linked to a significant presence of *Turborotalita quinqueloba*. These factors have been associated with different sea surface water masses: warm and salty surface waters like the NAC water (factor 1), cold and low saline surface waters similar to the Arctic water (factor 2), and the Arctic front water, which is the boundary between Atlantic and Arctic water (factor 3).

The high resolution study of the planktic foraminifer assemblages of Site U1314, their factor analysis, and a synthesis of Arctic front proxies (planktic foraminifer and diatom data) from other subpolar North Atlantic sites, allowed us to track the migrations of the AF over the studied interval (ca. 800–400 ka) and to track paleoceanographic changes in North Atlantic surface circulation. Moreover, the combination of the inferred sea surface circulation changes with a synthesis of North Atlantic deep ocean circulation and ice volume changes during the 800–400 ka interval led us to divide each climatic cycle in five phases: early interglacial periods, late interglacial periods, first phase of glacial periods, second phase of glacial periods and third phase of glacial periods.

During the early interglacial phase the transitional and subpolar species dominated the assemblage at all the sites mentioned (with abundances above 65% at Site U1314). Those warm conditions indicated that the Arctic front position and surface water masses distribution were similar to present day and so the PF. The NAC, warm and with high salinity, reached the Labrador Sea (via the IC) and the NGS where it cooled and sank to generate NADW.

During the late interglacial periods minor to moderate increases in *N. pachyderma* sin and *T. quinqueloba* abundances in the western North Atlantic indicate that the AF gradually moved southeastwards. It is likely that low insolation enhanced sea ice growth in the Arctic, promoting sea ice export through the EGC (Born et al., 2010) which reduced convection in the Labrador Sea and weakened the IC (Fig. 5b). However, the benthic δ^{18}O values suggest that ice sheets were not growing but still waning and the benthic δ^{13}C values suggested an active AMOC. The eastern North Atlantic remained warm due to the influence of the NAC and NADW formation was strong in the NGS.

During the first phase of glacial periods the rapid increase in *N. pachyderma* sin (above 65% at Site U1314) indicated that the AF shifted southwards of all sites but 980 (where *N. pachyderma* sin values remained low) which still was in the Atlantic waters (Fig. 5c). The lingering warm conditions in the eastern subpolar North Atlantic are linked to the continuous flow of the NAC that still reached the NGS and generated NADW. The high benthic δ^{13}C values support that the AMOC was still strong besides the ice sheet growth has already started (benthic δ^{18}O values began to increase in this phase). Sea ice export through the EGC was probably enhanced due to albedo and other factors that amplified the cooling trend triggered by the low insolation of the previous phase. Arctic waters expanded in the western subpolar North Atlantic dampening Labrador Sea deep water convection, which slightly reduced the AMOC (Born et al., 2010).

The second phase of the glacial periods began with a rapid return of the transitional-subpolar assemblage to the central and eastern subpolar North Atlantic associated with the first significant ice-rafting events recorded at Site U1314 (Wright and Flower, 2002; Alonso-Garcia et al., 2011). During this phase SSTs were predominantly warm reaching interglacial values during the warmest intervals, and the AF position was similar to the late interglacial phase (Fig. 5d). However, the ice volume was larger than in the late interglacial periods and this second phase is characterised by rapid SST changes linked to ice-rafting events. As a result of calving and meltwater discharges deep water convection in the NGS slowed down disturbing the AMOC (Alonso-Garcia et al., 2011). The retreat of the AF northwards of Site U1314 occurred as a consequence of the strong reduction of the AMOC during ice-rafting events, which led to the storage of huge amounts of warm water in the subsurface North Atlantic (Moros et al., 2002; Rasmussen and Thomsen, 2004; Alonso-Garcia et al., 2011).

The third phase of glacial periods corresponds to full glacial conditions in which *N. pachyderma* sin dominated the assemblage at all subpolar North Atlantic, even at site 980 (with relative abundances always over 65% and mostly over 80%). The AF was located almost east–west from Newfoundland to Ireland and the PF was between Sites 983 and U1314. During this phase the ice accumulated on the continents was large, deep ocean circulation shifted to the glacial mode in which Glacial North Atlantic intermediate water was generated and ice-rafting events were followed by moderately warm events.

During Terminations the AF rapidly moved northwestwards reaching a position similar to present. The North Atlantic surface water masses distribution changed from the third glacial phase distribution to the early interglacial phase in a few thousand years.

Acknowledgements

Thanks to IODP for providing the samples and maps (thank K. Petronotis). Thanks to A. Cortina and K. Radabaugh for their help with statistics and writing. This study was funded by the research projects CGL2005-00642/BTE, CGL2006-10593, CGL2008-05560, as well as the Ministry of Education and Science project GRACCIE (CONSOLIDER-INGENIO CSD 2007–00067) and Junta de Castilla y León funding (Grupo de excelencia GR34). Support from the Spanish government through a FPU fellowship (AP-2005-2805) granted to Montserrat Alonso-García is gratefully acknowledged.

Appendix A. Supplementary data

Supplementary data to this article can be found online at doi:10.1016/j.palaeo.2011.09.004.

References

Aksu, A.E., de Vernal, A., Mudie, P.J., 1989. High-resolution foraminifer, palynologic, and stable isotopic records of upper Pleistocene sediments from the Labrador Sea: paleoclimatic and paleoceanographic trends. In: Srivastava, S.P., Arthur, M., Clement, B. (Eds.), Proceedings of the Ocean Drilling Program, Scientific results, vol. 105. Ocean Drilling Program, College Station, TX, pp. 617–652.

Aksu, A.E., Mudie, P.J., de Vernal, A., Gillespie, H., 1992. Ocean–atmosphere responses to climatic change in the Labrador Sea: Pleistocene plankton and pollen records. Palaeogeogr. Palaeoclimatol. Palaeoecol. 92, 121–138.

Alonso-Garcia, M., Sierro, F.J., Kucera, M., Flores, J.A., Cacho, I., Andersen, N., 2011. Ocean circulation, ice sheet growth and interhemispheric coupling of millennial climate variability during the mid-Pleistocene (ca. 800–96400 ka). Quaternary Science Reviews 30, 3234–3247.

Bauch, D., Carstens, J., Wefer, G., 1997. Oxygen isotope composition of living Neogloboquadrina pachyderma (sin.) in the Arctic Ocean. Earth and Planetary Science Letters 146, 47–58.

Bé, A.W.H., 1977. An ecological, zoogeographic and taxonomic review of recent planktonic foraminifera. In: Ramsay, A.T.S. (Ed.), Oceanic Micropalaeontology. Academic Press, London, pp. 1–100.

Bé, A.W.H., Tolderlund, D.S., 1971. Distribution and ecology of living planktonic foraminifera in surface waters of the Atlantic and Indian Oceans. In: Funnell, B., Riedel, W.R. (Eds.), The Micropaleontology of the Oceans. Cambridge University Press, London, pp. 105–149.

Berger, W.H., Jansen, E., 1994. Mid-Pleistocene climate shift — the Nansen connection. In: Johannessen, O.M., Muench, R.D., Overland, J.E. (Eds.), The Polar Oceans and their Role in Shaping the Global Environment. AGU, Washington D.C., pp. 295–311.

Berger, W.H., Wefer, G., 2003. On the dynamics of the ice ages: stage-11 paradox, mid-brunhes climate shift, and 100-ky cycle. In: Droxler, A.W., Poore, R.Z., Burkle, L.H. (Eds.), Earth's climate and orbital eccentricity. the marine isotope stage 11 question. Geophysical Monograph, vol. 137. Americal Geophysical Union, Washington D.C, pp. 41–59.

Bianchi, G.G., McCave, I.N., 2000. Hydrography and sedimentation under the deep western boundary current on Björn and Gardar Drifts, Iceland Basin. Mar. Geol. 165, 137–169.

Bonelli, S., Charbit, S., Kageyama, M., Woillez, M.N., Ramstein, G., Dumas, C., Quiquet, A., 2009. Investigating the evolution of major Northern Hemisphere ice sheets during the last glacial–interglacial cycle. Climate of the Past 5, 329–345.

Born, A., Levermann, A., Mignot, J., 2009. Sensitivity of the Atlantic Ocean circulation to a hydraulic overflow parameterisation in a coarse resolution model: Response of the subpolar gyre. Ocean Modelling 27, 130–142.

Born, A., Nisancioglu, K., Braconnot, P., 2010. Sea ice induced changes in ocean circulation during the Eemian. Clim. Dyn. 35, 1361–1371.

Boyle, E.A., Keigwin, L.D., 1982. Deep circulation of the North Atlantic over the last 200,000 years: geochemical evidence. Science 218, 784–787.

Boyle, E.A., Keigwin, L., 1987. North Atlantic thermohaline circulation during the past 20,000 years linked to high-latitude surface temperature. Nature 330, 35–40.

Broecker, W.S., 1991. The great ocean conveyor. Oceanography 4, 79–89.

Broecker, W.S., Denton, G.H., 1989. The role of ocean–atmosphere reorganizations in glacial cycles. Geochimica et Cosmochimica Acta 53, 2465–2501.

Broecker, W., Peng, T.-H., 1989. The Cause of the Glacial to Interglacial Atmospheric CO 2 Change: A Polar Alkalinity Hypothesis. Broecker, W., and E. Maier-Reimer (1992), The Influence of Air and Sea Exchange on the Carbon Isotope Distribution in the Sea, Global Biogeochem. Cycles, 6(3), 315–320. 3, 215–239.

Carstens, J., Wefer, G., 1992. Recent distribution of planktonic foraminifera in the Nansen Basin. Arctic Ocean. Deep Sea Research Part A. Oceanographic Research Papers 39, S507–S524.

Channell, J.E.T., Kanamatsu, T., Sato, T., Stein, R., Alvarez Zarikian, C.A., Malone, M.J., Scientists, t.E., 2006. 303/306 Expedition reports, North Atlantic Climate. Proceedings of the Integrated Ocean Drilling Program, College Station TX (Integrated Ocean Drilling Program Management International, Inc.).

Clark, P.U., Archer, D., Pollard, D., Blum, J.D., Rial, J.A., Brovkin, V., Mix, A.C., Pisias, N.G., Roy, M., 2006. The middle Pleistocene transition: characteristics, mechanisms, and implications for long-term changes in atmospheric pCO2. Quat. Sci. Rev. 25, 3150–3184.

Coplen, T.B., 1996. More uncertainty than necessary. Paleoceanography 11, 369–370. doi:10.1029/1096PA01420.

Cortijo, E., Duplessy, J.C., Labeyrie, L., Leclaire, H., Duprat, J., van Wearing, T.C.E., 1994. Eemian cooling in the Norwegian Sea and North Atlantic ocean preceding continental ice-sheet growth. Nature 372, 446–449.

Crucifix, M., Loutre, F., 2002. Transient simulations over the last interglacial period (126–115 kyr BP): feedback and forcing analysis. Clim. Dyn. 19, 417–433.

Curry, W.B., Lohmann, G.P., 1983. Reduced advection into Atlantic Ocean deep eastern basins during last glaciation maximum. Nature 306, 577–580.

Curry, W.B., Oppo, D.W., 2005. Glacial water mass geometry and the distribution of δ 13 C of Sigma CO 2 in the western Atlantic Ocean. Paleoceanography 20, 1–12.

Curry, W., Duplessy, J., Labeyrie, L., Shackleton, N., 1988. Changes in the distribution of δ13C of deep water ΣCO 2 between the Last Glaciation and the Holocene. Paleoceanography 3, 317–341.

Denton, G.H., Alley, R.B., Comer, G.C., Broecker, W.S., 2005. The role of seasonality in abrupt climate change. Quat. Sci. Rev. 24, 1159–1182.

Denton, G.H., Anderson, R.F., Toggweiler, J.R., Edwards, R.L., Schaefer, J.M., Putnam, A.E., 2010. The Last Glacial Termination. Science 328, 1652–1656.

Dickson, R.R., Gmitrowicz, E.M., Watson, A.J., 1990. Deep-water renewal in the northern North Atlantic. Nature 344, 848–850.

Dietrich, G., 1969. Atlas of the hydrography of the Northern Atlantic Ocean based on the Polar Front Survey of the International Geophysical Year, winter and summer 1958. Copenhagen.

Duplessy, J.C., Shackleton, N.J., Fairbanks, R.G., Labeyrie, L., Oppo, D., Kallel, N., 1988. Deepwater source variations during the last climatic cycle and their impact on the global deepwater circulation. Paleoceanography 3, 343–360.

Fraile, I., Schulz, M., Mulitza, S., Merkel, U., Prange, M., Paul, A., 2009. Modeling the seasonal distribution of planktonic foraminifera during the Last Glacial Maximum. Paleoceanography 24, PA2216. doi:10.1029/2008PA001686.

Fronval, T., Jansen, E., 1997. Eemian and Early Weichselian (140–60 ka) Paleoceanography and Paleoclimate in the Nordic Seas with comparisons to Holocene conditions. Paleoceanography 12, 443–462.

Fronval, T., Jansen, E., Haflidason, H., Sejrup, J.P., 1998. Variability in surface and deep water conditions in the Nordic seas during the last interglacial period. Quat. Sci. Rev. 17, 963–985.

Gildor, H., Tziperman, E., 2001. A sea ice climate switch mechanism for the 100-kyr glacial cycles. J. Geophys. Res. 106, 9117–9133. doi:10.1029/1999JC000120.

Hakkinen, S., Rhines, P.B., 2004. Decline of subpolar North Atlantic circulation during the 1990s. Science 304, 555–559.

Hansen, B., Østerhus, S., 2000. North Atlantic-Nordic Seas exchanges. Progress In Oceanography 45, 109–208.

Hatun, H., Sando, A.B., Drange, H., Hansen, B., Valdimarsson, H., 2005. Influence of the Atlantic subpolar gyre on the thermohaline circulation. Science 309, 1841–1844.

Helland-Hansen, B., Nansen, F., 1909. The Norwegian Sea. Its physical oceanography based upon the Norwegian researches 1900–1904. Reports on Norwegian Fishery and Marine investigations 2, 1–359.

Hemleben, C., Spindler, M., Anderson, O.R., 1989. Modern Planktonic Foraminifera. Springer-Verlag, New York.

Hernández-Almeida, I., Bjørklund, K.R., Sierro, F.J., Filippelli, G.M., Cacho, I., Flores, J.A., in press. A high resolution opal and radiolarian record from the subpolar North Atlantic during the Mid-Pleistocene Transition (1069–779 ka): palaeoceanographic implications. Palaeogeography, Palaeoclimatology, Palaeoecology. doi:10.1016/j.palaeo.2011.05.049.

Imbrie, J., 1963. Factor and vector analysis programs for analyzing geologic data, Office Naval Res. Geography Branch, Technical Rept. 6 (CNR Task No. 389–135), p. 83.

Imbrie, J., Berger, A., Boyle, E.A., Clemens, S.C., Duffy, A., Howard, W.R., Kukla, G., Kutzbach, J., Martinson, D.G., McIntyre, A., Mix, A.C., Molfino, B., Morley, J.J., Peterson, L.C., Pisias, N.G., Prell, W.L., Raymo, M.E., Shackleton, N.J., Toggweiler, J.R., 1993. On the structure and origin of major glaciation cycles 2. The 100,000-year cycle. Paleoceanography 8, 699–735.

Isarin, R.F.B., Renssen, H., Vandenberghe, J., 1998. The impact of the North Atlantic Ocean on the Younger Dryas climate in northwestern and central Europe. J. Quat. Sci. 13, 447–453.

Jansen, J.H.F., Kuijpers, A., Troelstra, S.R., 1986. A mid-brunhes climatic event: long-term changes in global atmosphere and ocean circulation. Science 232, 619–622.

Johannessen, T., Jansen, E., Flatoy, A., Ravelo, A.C., 1994. The relationship between surface water masses, oceanographic fronts and paleoclimatic proxies in surface sediments of the Greenland, Iceland, Norwegian seas. In: Zahn, R., Pederesen, T.F., Kaminski, M.A., Labeyrie, L. (Eds.), Carbon cycling in the glacial ocean. *NATO ASI Series*, vol. I. Springer-Verlag, Berlin Heidelberg, p. 580.

Jonkers, L., Brummer, G.-J.A., Peeters, F.J.C., van Aken, H.M., De Jong, M.F., 2010. Seasonal stratification, shell flux, and oxygen isotope dynamics of left-coiling N. pachyderma and T. quinqueloba in the western subpolar North Atlantic. Paleoceanography 25, PA2204.

Koç, N., Flower, B.P., 1998. High-resolution Pleistocene diatom biostratigraphy and paleoceanography of Site 919 from the Irminger Basin. In: Saunders, A.D., Larsen, H.C., Wise Jr., S.W. (Eds.), Proceedings of the Ocean Drilling Program, Scientific Results, 152. College Station, TX (Ocean Drilling Program), pp. 209–219.

Koç, N., Hodell, D.A., Kleiven, H.F., Labeyrie, L., 1999. High-resolution Pleistocene diatom biostratigraphy of Site 983 and correlations with isotope stratigraphy. In: Raymo, M.E., Jansen, E., Blum, P., Herbert, T. (Eds.), Proceedings of the Ocean Drilling Program, Scientific Results, 162. College Station, TX (Ocean Drilling Program), pp. 51–62.

Kucera, M., Weinelt, M., Kiefer, T., Pflaumann, U., Hayes, A., Weinelt, M., Chen, M.-T., Mix, A.C., Barrows, T.T., Cortijo, E., Duprat, J., Juggins, S., Waelbroeck, C., 2005. Reconstruction of sea-surface temperatures from assemblages of planktonic foraminifera: multi-technique approach based on geographically constrained calibration data sets and its application to glacial Atlantic and Pacific Oceans. Quat. Sci. Rev. 24, 951–998.

Landais, A., Masson-Delmotte, V., Jouzel, J., Raynaud, D., Johnsen, S., Huber, C., Leuenberger, M., Schwander, J., Minster, B., 2006. The glacial inception as recorded in the NorthGRIP Greenland ice core: timing, structure and associated abrupt temperature changes. Clim. Dyn. 26, 273–284.

Lisiecki, L.E., Raymo, M.E., 2005. A Pliocene–Pleistocene stack of globally distributed benthic δ18O records. Paleoceanography 20. doi:10.1029/2004PA001071.

Loulergue, L., Schilt, A., Spahni, R., Masson-Delmotte, V., Blunier, T., Lemieux, B., Barnola, J.-M., Raynaud, D., Stocker, T.F., Chappellaz, J., 2008. Orbital and millennial-scale features of atmospheric CH4 over the past 800,000 years. Nature 453, 383–386.

Luthi, D., Le Floch, M., Bereiter, B., Blunier, T., Barnola, J.-M., Siegenthaler, U., Raynaud, D., Jouzel, J., Fischer, H., Kawamura, K., Stocker, T.F., 2008. High-resolution carbon dioxide concentration record 650,000–800,000 years before present. Nature 453, 379–382.

Malmgren, B.r.A., Kucera, M., Nyberg, J., Waelbroeck, C., 2001. Comparison of statistical and artificial neural network techniques for estimating past sea surface temperatures from planktonic foraminifer census data. Paleoceanography 16, 520–530.

Marchitto, T.M., Broecker, W.S., 2006. Deep water mass geometry in the glacial Atlantic Ocean: a review of constraints from the paleonutrient proxy Cd/Ca. Geochemistry, Geophysics, Geosystems 7, Q12003.

Maslin, M.A., Ridgwell, A.J., 2005. Mid-Pleistocene revolution and the ‘eccentricity myth’. Geological Society, London, Special Publications 247, 19–34.

McClymont, E.L., Rosell-Melé, A., Haug, G.H., Lloyd, J.M., 2008. Expansion of subarctic water masses in the North Atlantic and Pacific oceans and implications for mid-Pleistocene ice sheet growth. Paleoceanography 23.

McManus, J.F., Oppo, D.W., Keigwin, L.D., Cullen, J.L., Bond, G.C., 2002. Thermohaline circulation and prolonged interglacial warmth in the North Atlantic. Quat. Res. 58, 17–21.

Miao, Q., Thunell, R.C., Anderson, D.M., 1994. Glacial–Holocene carbonate dissolution and sea surface temperatures in the South China and Sulu Seas. Paleoceanography 9, 269–290.

Moros, M., Kuijpers, A., Snowball, I., Lassen, S., Bäckström, D., Gingele, F., McManus, J., 2002. Were glacial iceberg surges in the North Atlantic triggered by climatic warming? Mar. Geol. 192, 393–417.

Mudelsee, M., Schulz, M., 1997. The Mid-Pleistocene climate transition: onset of 100 ka cycle lags ice volume build-up by 280 ka. Earth and Planetary Science Letters 151, 117–123.

Mudelsee, M., Stattegger, K., 1997. Exploring the structure of the mid-Pleistocene revolution with advanced methods of time-series analysis. Geol. Rundsch. 86, 499–511.

Nyland, B.F., Jansen, E., Elderfield, H., Andersson, C., 2006. Neogloboquadrina pachyderma (dex. and sin.) Mg/Ca and d18O records from the Norwegian Sea. Geochemistry, Geophysics, Geosystems 7, Q10P17. doi:10.1029/2005GC001055.

Oerlemans, J., 1984. On the origin of the ice ages. In: Berger, A., Hays, J.I.H., Kukla, G., Saltzman, B. (Eds.), Milankovitch and Climate, Part 2. D. Reidel, Norwell, MA, pp. 607–611.

Oppo, D.W., Fairbanks, R.G., 1987. Variability in the deep and intermediate water circulation of the Atlantic Ocean during the past 25,000 years: Northern Hemisphere modulation of the Southern Ocean. Earth and Planetary Science Letters 86, 1–15.

Oppo, D.W., Keigwin, L.D., McManus, J.F., Cullen, J.L., 2001. Persistent suborbital climate variability in marine isotope stage 5 and termination II. Paleoceanography 16, 280–292.

Oppo, D.W., McManus, J.F., Cullen, J.L., 2006. Evolution and demise of the Last Interglacial warmth in the subpolar North Atlantic. Quat. Sci. Rev. 25, 3268–3277.

Paillard, D., 1998. The timing of Pleistocene glaciations from a simple multiple-state climate model. Nature 391, 378–381.

Pflaumann, U., Sarnthein, M., Chapman, M., d'Abreu, L., Funnell, B., Huels, M., Kiefer, T., Maslin, M., Schulz, H., Swallow, J., van Kreveld, S., Vautravers, M., Vogelsang, E., Weinelt, M., 2003. Glacial North Atlantic: sea-surface conditions reconstructed by GLAMAP 2000. Paleoceanography 18, 1065. doi:10.1029/2002PA000774.

Pisias, N.G., Moore Jr., T.C., 1981. The evolution of Pleistocene climate: a time series approach. Earth and Planetary Science Letters 52, 450–458.

Rasmussen, T.L., Thomsen, E., 2004. The role of the North Atlantic Drift in the millennial timescale glacial climate fluctuations. Palaeogeogr. Palaeoclimatol. Palaeoecol. 210, 101–116.

Raymo, M.E., Oppo, D.W., Curry, W.B., 1997. The mid-Pleistocene climate transition: a deep sea carbon isotopic perspective. Paleoceanography 12, 546–559.

Reynolds, L., Thunell, R.C., 1985. Seasonal succession of planktonic foraminifera in the subpolar North Pacific. J. Foraminifer. Res. 15, 282–301.

Rial, J.A., 2004. Earth's orbital eccentricity and the rhythm of the Pleistocene ice ages: the concealed pacemaker. Glob. Planet. Chang. 41, 81–93.

Ruddiman, W.F., McIntyre, A., 1979. Warmth of the subpolar North Atlantic Ocean during Northern Hemisphere ice-sheet growth. Science 204, 173–175.

Ruddiman, W.F., McIntyre, A., 1981. Oceanic mechanisms for amplification of the 23,000-year ice-volume cycle. Science 212, 617–627.

Ruddiman, W.F., McIntyre, A., Niebler-Hunt, V., Durazzi, J.T., 1980. Oceanic evidence for the mechanism of rapid northern hemisphere glaciation. Quat. Res. 13, 33–64.

Schmitz, W.J., McCartney, M., 1993. On the North Atlantic circulation. Rev. Geophys. 31, 29–49.

Shimada, C., Sato, T., Toyoshima, S., Yamasaki, M., Tanimura, Y., 2008. Paleoecological significance of laminated diatomaceous oozes during the middle-to-late Pleistocene, North Atlantic Ocean (IODP Site U1304). Mar. Micropaleontol. 69, 139–150.

Siegenthaler, U., Stocker, T.F., Monnin, E., Luthi, D., Schwander, J., Stauffer, B., Raynaud, D., Barnola, J.-M., Fischer, H., Masson-Delmotte, V., Jouzel, J., 2005. Stable carbon cycle–climate relationship during the late Pleistocene. Science 310, 1313–1317.

Simstich, J., Sarnthein, M., Erlenkeuser, H., 2003. Paired d18O signals of Neogloboquadrina pachyderma (s) and Turborotalita quinqueloba show thermal stratification structure in Nordic Seas. Mar. Micropaleontol. 48, 107–125.

St. John, K., Flower, B.P., Krissek, L., 2004. Evolution of iceberg melting, biological productivity, and the record of Icelandic volcanism in the Irminger basin since 630 ka. Mar. Geol. 212, 133–152.

Stangeew, E., 2001. Distribution and isotopic composition of living planktonic foraminifera N. pachyderma (sinistral) and T. quinqueloba in the high latitude North Atlantic, Ph.D. dissertation, Mathematisch-Naturwissenschaftliche Fakultät. Christian-Albrechts-Universität, Kiel, Germany, p. 98.

Swift, J., 1986. The Arctic waters. In: Hurdle, B.G. (Ed.), The Nordic Seas. Springer, New York, pp. 129–151.

Swift, J.H., Aagaard, K., 1981. Seasonal transitions and water mass formation in the Iceland and Greenland seas. Deep Sea Research Part A. Oceanographic Research Papers 28, 1107–1129.

Thunell, R.C., 1976. Optimum indices of calcium carbonate dissolution, in deep-sea sediments. Geology 4, 525–528.

Tolderlund, D.S., Bé, A.W.H., 1971. Seasonal distribution of planktonic foraminifera in the western North Atlantic. Micropaleontology 17, 297–329.

Tomczak, M., Godfrey, J.S., 1994. Regional Oceanography: an Introduction. Pergamon, London.

Tzedakis, P.C., 2005. Towards an understanding of the response of southern European vegetation to orbital and suborbital climate variability. Quat. Sci. Rev. 24, 1585–1599.

Tzedakis, P.C., Raynaud, D., McManus, J.F., Berger, A., Brovkin, V., Kiefer, T., 2009. Interglacial diversity. Nat. Geosci. 2, 751–755.

Tziperman, E., Gildor, H., 2003. On the mid-Pleistocene transition to 100-kyr glacial cycles and the asymmetry between glaciation and deglaciation times. Paleoceanography 18, 1001 1010.1029/2001pa000627.

Venz, K.A., Hodell, D.A., Stanton, C., Warnke, D.A., 1999. A 1.0 Myr record of Glacial North Atlantic intermediate water variability from ODP site 982 in the northeast Atlantic. Paleoceanography 14, 42–52.

Wang, Z., Mysak, L.A., 2002. Simulation of the last glacial inception and rapid ice sheet growth in the McGill paleoclimate model. Geophys. Res. Lett. 29, 2102.

Wright, A.K., Flower, B.P., 2002. Surface and deep ocean circulation in the subpolar North Atlantic during the mid-Pleistocene revolution. Paleoceanography 17, 1068.